Journal of Applied Polymer Science

Improvement in Mechanical and Thermal Properties of Phenolic Foam Reinforced with Multiwalled Carbon Nanotubes

Zhongjia Yang, Lili Yuan, Yizhuo Gu, Min Li, Zhijie Sun, Zuoguang Zhang
Key Laboratory of Aerospace Materials and Performance (Ministry of Education), School of Materials Science and Engineering, Beihang University, Beijing 100191, People's Republic of China
Correspondence to: Y. Gu (E-mail: benniegu@buaa.edu.cn).

ABSTRACT: Phenolic foams reinforced with pristine and functionalized multiwalled carbon nanotubes (MWCNTs) were fabricated to develop fire-resistant materials with improved mechanical properties. The influences of the contents of carboxyl multi-walled carbon nanotubes (MWCNTs-COOH) and of MWCNTs types on the compressive properties of the composite foams were investigated. The microstructure and detailed failure behavior of MWCNTs/phenolic composite foams were studied using scanning electron microscopy (SEM) and *in situ* quasistatic compression inside SEM, respectively. In addition, thermal performances were evaluated by thermogravimetric analysis (TGA) and vertical burning method. It is found that as heterogeneous nucleation agents, MWCNTs increase cell density and decrease cell size of the produced foams, and that as reinforcements located in cell walls, MWCNTs impart high strength and stiffness to brittle foams. Moreover, MWCNTs reinforced foams have higher thermal stability than raw foams and exhibit similar excellent resistance to flame, confirming the effectiveness of MWCNTs as stabilizers. © 2013 Wiley Periodicals, Inc. J. Appl. Polym. Sci. 130: 1479–1488, 2013

KEYWORDS: foams; flame retardance; mechanical properties

Received 8 October 2012; accepted 26 March 2013; Published online 26 April 2013
DOI: 10.1002/app.39326

INTRODUCTION

Unlike those market-leading polymeric foams as polyvinyl chloride (PVC), polystyrene (PS), and polyurethane (PU) foams, phenolic foam exhibits excellent comprehensive thermal properties, including low thermal conductivity coefficient, flame resistance without incorporating any fire-retardant additives, i.e., nondripping during combustion, low smoke density and smoke toxicity, as well as thermal stability over a broad temperature range.[1,2] As a consequence, phenolic foam has been the leading candidate in a wide range of applications with stringent requirements for flame, smoke, and toxicity, like civil construction, chemical industry, and aerospace application.[3,4] However, one of the main drawbacks of phenolic foam, particularly that of low density, is intrinsically brittle due to the structure of its molecular chain,[5] which causes low strength, poor impact resistance, and high friability. This leads to serious problems such as skin debonding in sandwich structure, susceptibility to damage during handling and dust pollution in workspace, thereby severely restricting its applications in engineering.[6–8]

Over the past few decades, there have been many attempts to make phenolic foam stronger and tougher, and these fall into two categories: chemical modification[5,9–11] and nonreactive approaches.[12–17] Incorporating chemical modifier, such as polyisocyanate,[5,9] polyacrylamide,[10] and glutaraldehyde,[11] is effective for improving the mechanical properties of phenolic foam, but deteriorates its flame retardancy. On the other hand, adding inert filler, like talc, mica, clay,[12,13] glass and ceramic miroballoons, fly ash,[14] etc., has shown to enhance the texture and homogeneity of foam, while increases the viscosity of the resin before foaming, and thus makes foams heavier. The incorporation of chopped fibers, including glass fiber, aramid fibers (e.g., Nomex and Kevlar)[15,16] and natural fibers (bamboo and cellulose fiber)[17] increases foam strength, stiffness, resistance to abrasion and dimensional stability. Although these fiber reinforcements are distinctly effective for the enhancement in the mechanical properties of phenolic foam, they affect the mixing and foaming process, leading to increased density and poor surface quality.

Since first reported by Sumio Iijima in 1991, carbon nanotubes (CNTs) have received increasing attention. With low density, large aspect ratio, and remarkable mechanical, electrical and thermal properties, CNTs provide lightweight, strong and high toughness characteristics to composites.[18,19] Until recently, researches regarding CNTs reinforced polymeric foams have been reported mainly referring to thermoplastic polymeric foams.[20–22] Small amounts of uniformly dispersed CNTs in a

polymer matrix as heterogeneous nucleation agents, can facilitate nucleating cells, leading to an alteration in the microstructure of foam, such as cell size and cell density.[20] Chen et al.[21] studied the influence of multiwalled carbon nanotubes (MWCNTs) aspect ratio on the morphology of the nanocomposite foam, and found that smaller aspect ratio yielded higher cell density under the same formulation and foaming process. Furthermore, strong interfacial interaction between functionalized CNTs and foam matrix improves the efficiency of stress transfer as well as the modulus and strength of the composite foam. The effect of MWCNTs on the mechanical properties of MWCNTs/PMMA nanocomposite foam was also revealed by Chen.[22] When MWCNTs concentration reached 1% by weight, Young's modulus of polymeric foam increased by 82%, and the collapse strength increased by 104%. Remarkable enhancement in tensile properties was observed when MWCNTs were added into ethylene vinyl acetate (EVA) foams.[23] Moreover, Zhang et al.[24] studied the mechanical behaviors of rigid polyurethane foam reinforced with MWCNTs, showing the effectiveness of CNTs on the compressive properties of thermoset foam.

In addition, multifunctional CNTs/polymeric composite foams are gaining intensive significance. For instance, Verdejo et al.[25] prepared MWCNTs/flexible polyurethane composite foam, and concluded that MWCNTs with the addition of 0.1 wt % enhanced the acoustic activity. MWCNTs reinforced poly (ε-caprolactone) (PCL)[26] and PS[27] foams showed extraordinary electromagnetic shielding (EMI) properties due to high electrical conductivity of CNTs. Besides, CNTs, acting as flame-retardant additives, demonstrate potential flammability reduction in many polymers, like polypropylene (PP),[28] PMMA,[29] and PS.[30] Many works have shown the advantages of CNTs reinforced foam, but few studies on CNTs/phenolic foam have been reported. Because the effect of CNTs on the properties of brittle foam is still not fully understood, the mechanical and functional performances of the nanocomposite foam are worth investigating.

This current article is aimed at showing the simultaneous enhancement in mechanical and thermal properties of phenolic foams via the inclusion of MWCNTs. Pristine, carboxyl, and amino MWCNTs were respectively well dispersed into phenolic resins through ultrasonic irradiation and MWCNTs reinforced phenolic foams were obtained by batch foaming process. The cell morphology, with and without MWCNTs additives, was observed by scanning electron microscopy (SEM). The influence of MWCNTs on the compressive properties of the composite foam was investigated, and *in situ* compression inside SEM was conducted to explore the reinforcing mechanism of MWCNTs. Moreover, thermal stability and flame-resistant property of these foams were analyzed by means of thermogravimetric analysis (TGA) and vertical burning test, respectively.

EXPERIMENTAL

Materials

Phenolic resolve resin (solid content = of 75–80%) was supplied by Shandong Shengquan Chemical. Both Tween-80 as surfactant and *n*-pentane as blowing agent were acquired from Xilong Chemical factory. Phosphoric and *p*-toluenesulfonic acid supplied by Beijing Yili Chemical were used as curing agents. Three kinds of MWCNTs, *i.e.*, pristine MWCNTs (*p*-MWCNTs), carboxyl MWCNTs (MWCNTs-COOH), and amino MWCNTs (MWCNTs-NH_2), of which the outer diameters were 20–30 nm and the lengths were 10–30 μm, were purchased from Chengdu Organic Chemicals. Alcohol, as the dispersion solvent for MWCNTs was obtained from Beijing Chemical Works.

Preparation of MWCNTs/Phenolic Composite Foam

All phenolic foam samples were synthesized in our laboratory through a proprietary formulation.[31] Manufacturing of MWCNTs/phenolic composite foam is a three-step process as shown in Figure 1. In step 1, phenolic resolve resin was mixed in a beaker with a small amount of surfactant and alcohol solution. After mechanical mixing, a certain amount of MWCNTs was dispersed in a phenolic solution with a high intensity ultrasonic horn (Ti-horn, power 800W, frequency 20 kHz) for several hours to make a stable suspension of MWCNTs. The appropriate sonication time was determined based on MWCNTs concentration. The mixing of samples containing 0.01, 0.03, and 0.05 wt % MWCNTs-COOH took 1, 2.5, and 4 h respectively. Next, MWCNTs dispersive solution was placed in a vacuum oven at 25°C for 6 h to remove alcohol. In step 2, blowing agent was added to the mixture, followed by being stirred mildly until no more free liquid was visible. Curing agents were then added into the creamy mixture and stirred for 30 s at 25°C. Finally, in step 3, the reacting mixture was quickly poured

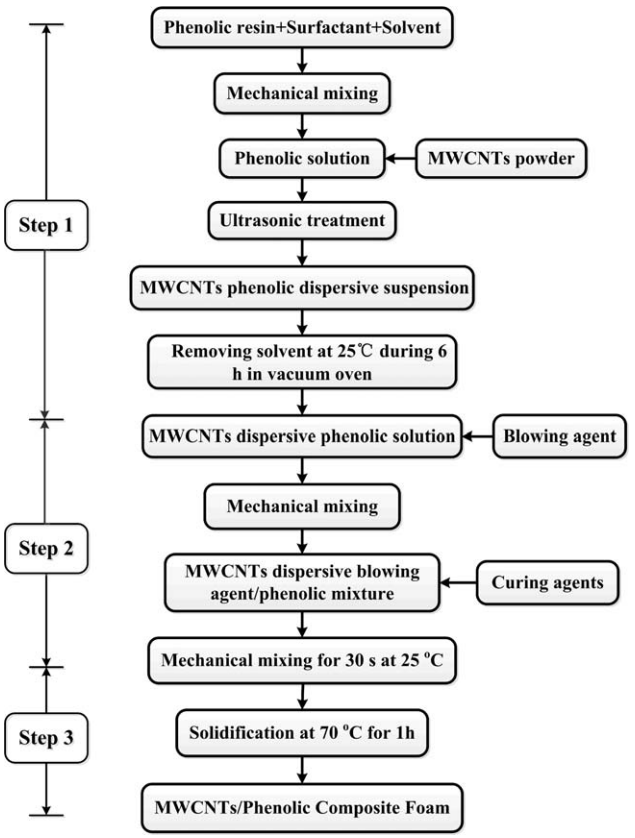

Figure 1. Preparation process for MWCNTs/phenolic composite foam.

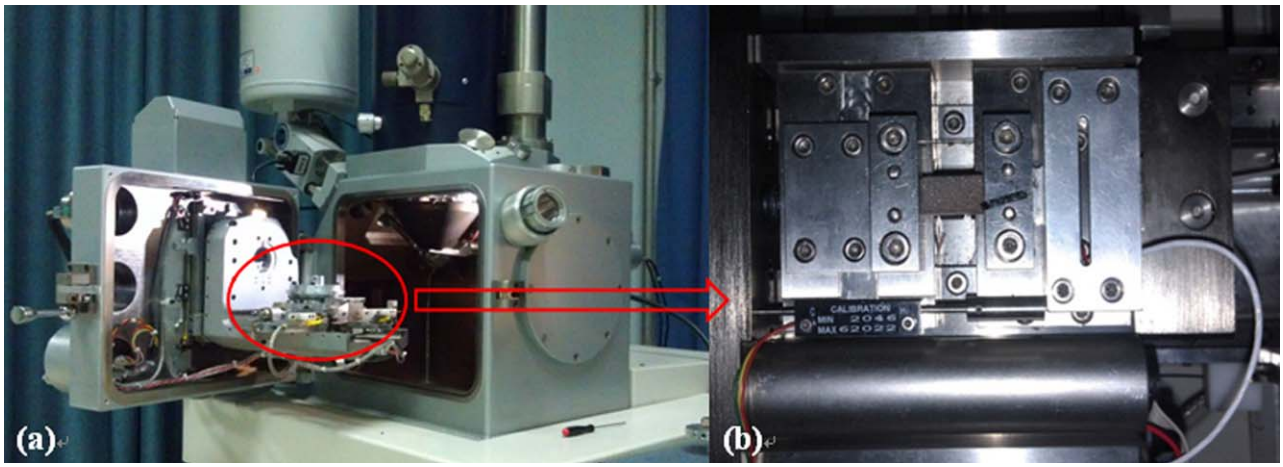

Figure 2. *In situ* quasistatic compression test equipment. [Color figure can be viewed in the online issue, which is available at wileyonlinelibrary.com.]

into a mould, and cured inside an oven at 70°C for 1 h to obtain MWCNTs/phenolic composite foam.

Characterizations of Phenolic Foam

Cell Structure. The structure of phenolic foam, including cell size $\bar{d}$ and cell density N_f, was examined by scanning electron microscopy (SEM, CamScan3400), and analyzed by means of Scion Image software. The samples from MWCNTs/phenolic composite foams were cut by a sharp surgical blade and then sputter-coated with gold to preclude charge build-up by electron absorption. Cell size $\bar{d}$ was calculated by the following equation[32]:

$$\bar{d} = L\frac{\sum_{i=0}^{i} N_i d_i}{\sum_{i=0}^{i} N_i} \quad (1)$$

where L was the proportional scale, and N_i was the number of cells with the apparent cell diameter d_i in μm. Cell density N_f was calculated by the following equation[33]:

$$N_f = \left(\frac{NM^2}{A}\right)^{3/2} \quad (2)$$

where A was the area of the micrograph, N was the number of cells with more than 50 cells chosen and M was the magnification factor. The thickness of cell face t_f was estimated by averaging the membrane thickness values of about 20 broken cells, and the thickness of cell wall t_e was determined by averaging the edge thickness in the same way.

The apparent density was measured from the sample weight in air, according to the China National Standard GB/T 6343-2009.

Mechanical Behavior. Compression testing, by means of a universal testing machine (UTM5000, Shenzhen SUNS), was carried out in accordance with China National Standard GB/T 8813-2008. Both MWCNTs composite foam and phenolic foam control samples were tailored to the dimensions of 60 mm × 60 mm × 30 mm and then compressed between two stainless steel platens with a crosshead speed of 0.5 mm min^{-1} until the samples deformed by 20%. Compressive strength was determined from the maximum load (in a range of strain $\leq$10%). Specific strength was used to exclude the influence of the difference in composite foam density on the mechanical properties, and was calculated by the following equation[34]:

$$\sigma_s = \frac{\sigma_m}{\rho_f \times 9.8} \quad (3)$$

where σ_m is compressive strength in kPa and ρ_f the apparent density of foam in g cm^{-3}.

In situ quasistatic compression test on specially designed small samples with dimensions of 12 mm × 5 mm × 12 mm was accomplished in a small loading device equipped inside SEM, which was designed to observe the overall collapse response of multiple cells corresponding to compression test on bulk foam, as illustrated in Figure 2. The samples were carefully sectioned from phenolic and MWCNTs/phenolic composite foams to avoid local damage to cell walls and cell faces, and then compressed along the horizontal direction (perpendicular to the observed direction by SEM) at a cross-head speed of 0.2 mm min^{-1} until 20% deformations were achieved. Microstructure series of cell deformation was investigated through SEM at an interval of every 3.3% deformation.

Thermal Properties. TGA (thermogravimetric analysis) was carried out on a NETZSCH STA449 F3 Jupiter to study the thermal stability of the as-prepared foams at a heating rate of 10°C min^{-1} from room temperature to 800°C under argon gas atmosphere. The samples about 5–10 mg were cut into small pieces by a surgical blade.

Flammability was assessed through vertical burning method in accordance with China National Standard GB/T 8333-2008, as illustrated in Figure 3. The tests were conducted on samples being cut from the as-fabricated foams with the dimensions of 12.7 mm × 10 mm × 10 mm. Each sample was mounted vertically on an iron support and ignited by an alcohol blast burner for 10 s, adjusting the flame cone 25-mm high. Loss of mass by entire specimen was recorded. To estimate the error and identify the repeatability of the test, six samples for each case were used to obtain the average loss of mass value.

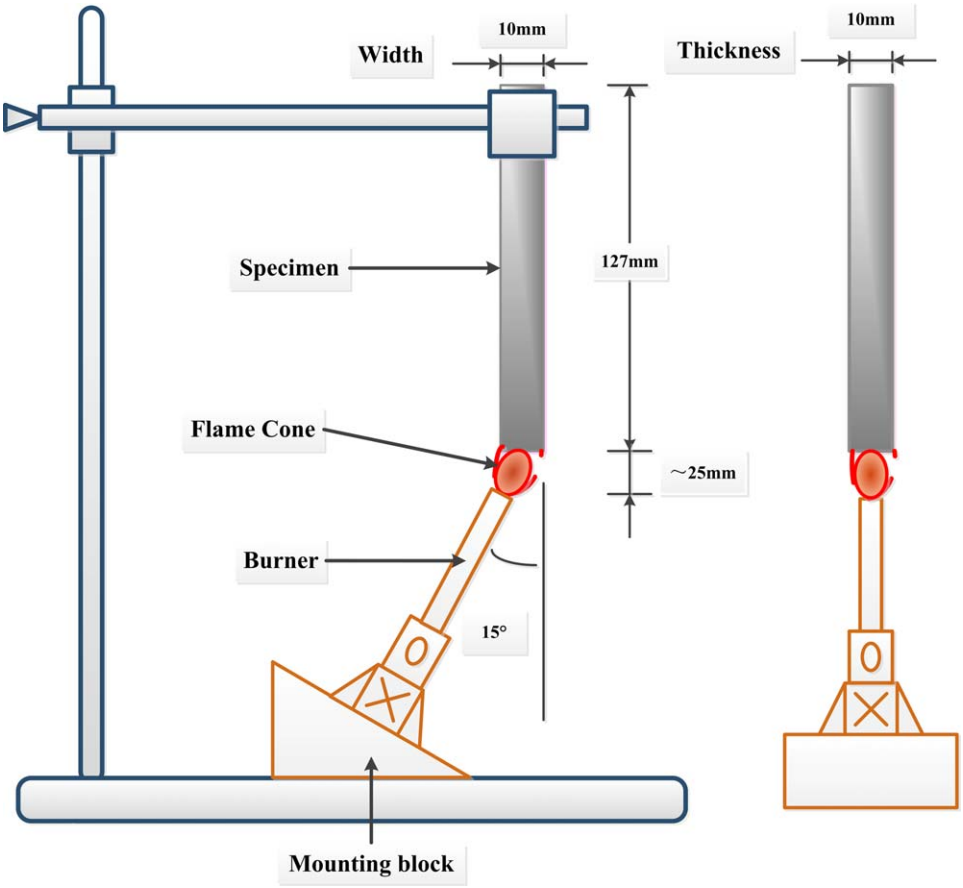

Figure 3. Test configuration and sample geometry of vertical burning method. [Color figure can be viewed in the online issue, which is available at wileyonlinelibrary.com.]

RESULTS AND DISCUSSION

Microstructure Characterization

Microstructures of phenolic and MWCNTs/phenolic composite foams are shown in Figure 4. It is observed that all foams exhibit closed-cell structures, and cell size and shape get uniform distribution over the region, which indicates a good dispersion of MWCNTs in phenolic resin during foaming process.

Table I shows the morphology parameters of MWCNTs/phenolic composite foams, compared to that of raw phenolic foam. It is clear that MWCNTs/phenolic composite foams have smaller average cell sizes and greater cell densities than those of phenolic foams. Furthermore, the average cell size of MWCNTs-COOH reinforced foams decreases with the increase of MWCNTs-COOH content, whereas the corresponding cell density increases as expected.[35] Nearly 32% decrease in cell size and 54% increase in cell density are achieved via the integration of 0.05 wt % MWCNTs-COOH into phenolic foam. This could be due to the fact that MWCNTs serve as heterogeneous nucleating agents during foaming stage which involves two basic steps, i.e., cell nucleation as well as cell growth and coalescence. In the first step, the well-dispersed MWCNTs lower the critical nucleation free energy,[21] implying that more cells begin to nucleate concurrently and less gases for cell growth accumulate on the phenolic resin/MWCNTs interfaces. In the second step, the interactions at the molecular level between MWCNTs and phenolic resin chains increase the viscosity of MWCNTs dispersive phenolic solution, thereby precluding cell growth.

As shown in Table II, all MWCNTs reinforced foams exhibit similar foam densities about 0.049 g cm^{-3}, showing a slight increment compared to the neat counterpart. This may well be attributed to the thickening of cell walls and shrinkage of cell space, as illustrated in Table I.

Compressive Properties

Effect of MWCNTs-COOH Content. Compression tests were conducted to study the effect of MWCNTs-COOH on the mechanical properties of the composite foams. A series of MWCNTs-COOH/phenolic foams with different mass fraction, including 0.01, 0.03, and 0.05 wt % were prepared.

The representative compressive stress–strain curves are shown in Figure 5. Phenolic foam exhibits a multistage deformation response when subjected to compressive loading, i.e., initial linear elasticity regime, controlled by the overall elastic bending of cell walls and stretching of cell faces; linear plateau region, depending on collapse of cells—on brittle crushing; and densification, accompanied by the complete collapse and contact between opposing cells, as described in Ref. 36. It can be seen that both compressive modulus and strength of MWCNTs-COOH/phenolic composite foams are evidently higher than

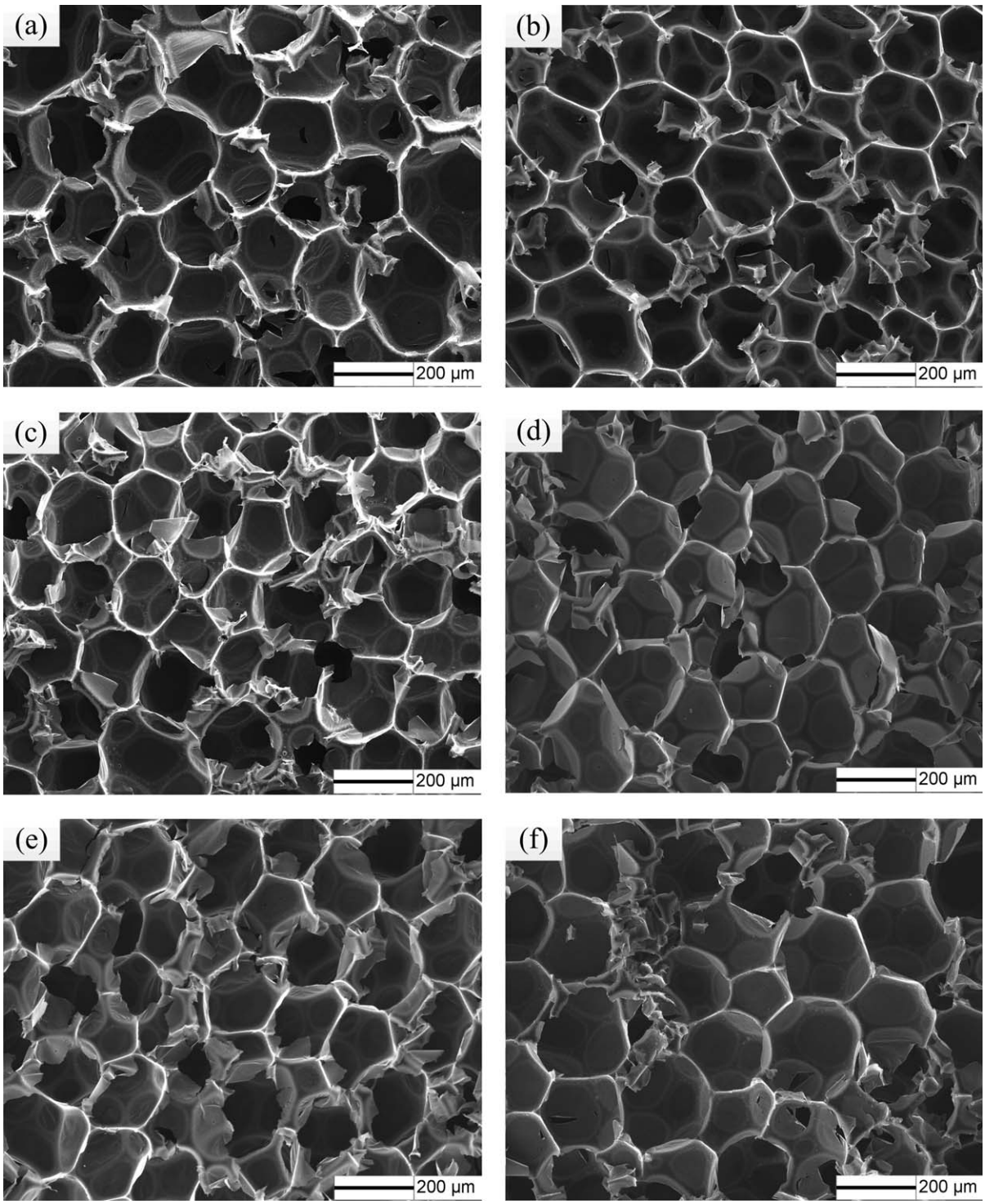

Figure 4. SEM images of phenolic foams under ×100 filled with: (a) 0.01 wt % MWCNTs-COOH; (b) 0.03 wt % MWCNTs-COOH; (c) 0.05 wt % MWCNTs-COOH; (d) 0.05 wt % *p*-MWCNTs; (e) 0.05 wt % MWCNTs-NH_2; (f) without MWCNTs.

Table I. Microcellular Structure of Phenolic and MWCNTs/Phenolic Composite Foams

Foam	Cell wall thickness, $t_e/\mu m$	Cell face thickness, t_f/nm	Cell size, $\bar{d}/\mu m$	Cell size rate-of-change (%)	Cell density, $N_f/\times 10^3$ cell/cm^3
Raw phenolic foam	13.5	520	244.4	0	6.98
0.01 wt % MWCNTs-COOH reinforced phenolic foam	16.4	490	216.9	−11.3	7.50
0.03 wt % MWCNTs-COOH reinforced phenolic foam	20	480	190.3	−22.1	8.40
0.05 wt % MWCNTs-COOH reinforced phenolic foam	18.5	438	165.8	−32.2	10.72
0.05 wt % MWCNTs-NH_2 reinforced phenolic foam	16.8	459	179	−26.8	9.89
0.05 wt % p-MWCNTs reinforced phenolic foam	16.5	424	172	−29.6	9.30

Table II. Compressive Properties of Phenolic and MWCNTs/Phenolic Composite Foams

Foam	Density (g cm^{-3})	Strength (MPa)	Specific strength (m)	Gain (%)
Raw phenolic foam	0.044	0.156	361	—
0.01 wt % MWCNTs-COOH reinforced phenolic foam	0.0504	0.174	353	−2
0.03 wt % MWCNTs-COOH reinforced phenolic foam	0.0477	0.202	431	19
0.05 wt % MWCNTs-COOH reinforced phenolic foam	0.0479	0.223	474	31
0.05 wt % MWCNTs-NH_2 reinforced phenolic foam	0.0503	0.209	424	18
0.05 wt % p-MWCNTs reinforced phenolic foam	0.0481	0.213	451	25

those of phenolic foams. As indicated in Table II, except for the composite foam containing 0.01 wt % MWCNTs-COOH, specific strength of the composite foam increases with the increment of MWCNTs-COOH content.

Effect of MWCNTs Type. Three kinds of MWCNTs/phenolic composite foams with mass fraction of 0.05% were made to investigate the influence of MWCNTs type. The influence of MWCNTs type on foam compressive strength is summarized in Table II and the corresponding stress–strain curves are shown in Figure 6. As expected, the addition of MWCNTs irrespective of MWCNTs type improves the compression modulus and strength relative to unreinforced foam; and MWCNTs-COOH reinforced foam shows the highest compressive properties. *In situ* compression tests in SEM for comparing *p*-MWCNTs/phenolic and MWCNTs-NH_2/phenolic composite foams with the neat system were carried out and similar trends in cell morphology to MWCNTs-COOH/phenolic composite foam were observed. This is attributed to that MWCNTs additions in cell walls impart high resistance to brittle fracture under compression loading, as previously discussed. In addition, the variations in foam properties reinforced by different kinds of MWCNTs are believed to arise from the differences in the interfacial compatibility between different MWCNTs and the matrix, which dominates the efficiency of interfacial load transfer.

Reinforcing Mechanism of MWCNTs. To understand the interactions among MWCNTs, cells and phenolic matrix, *in situ* compressive experiment inside SEM with a small loading attachment was employed via observing the evolution of cell morphology during deformation of 0.05 wt % MWCNTs-COOH/phenolic composite foam sample, compared with raw phenolic foam sample.

Figure 7 shows the deformation and failure morphology of raw phenolic foam subjected to compressive load. In Figure 7(a,b), cell walls bend and the membranes of cell faces stretch in accordance with progressively compressed enclosed spaces, corresponding to linear elastic deformation that is homogeneous through the sample. Surpassing the first maximum in stress, the deformation starts to localize. Within the localized band, as arriving at the modulus of rupture, brittle fracture initiates at weak cell walls so fast that SEM image could not be taken, while deformation apart from the band remains symmetric and homogeneous.[36] With the increasing strain, cracks in crushing cells propagate dramatically along the cells nearby, as presented in Figure 7(c); and eventually, the walls of collapsed opposing cells

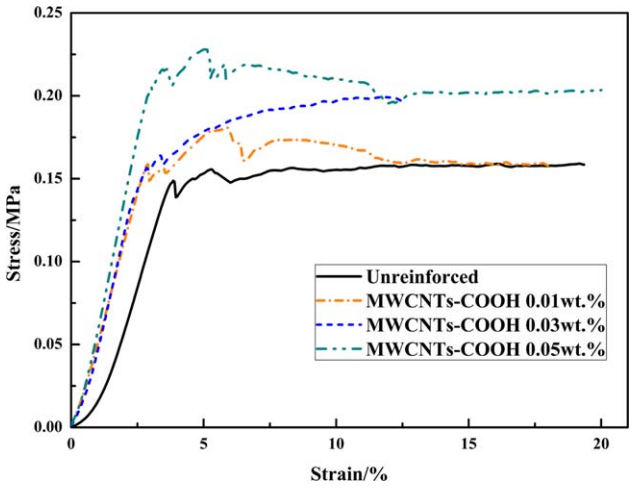

Figure 5. Typical compressive stress–strain curves of phenolic foams filled with MWCNTs-COOH under different mass fraction. Loading direction is parallel to the foam rise direction. [Color figure can be viewed in the online issue, which is available at wileyonlinelibrary.com.]

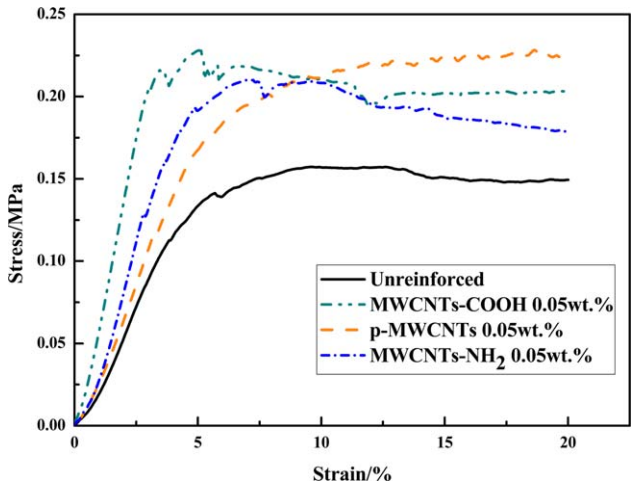

Figure 6. Typical compressive stress–strain curves of phenolic foams filled with MWCNTs in different types. Loading direction is parallel to the foam rise direction. [Color figure can be viewed in the online issue, which is available at wileyonlinelibrary.com.]

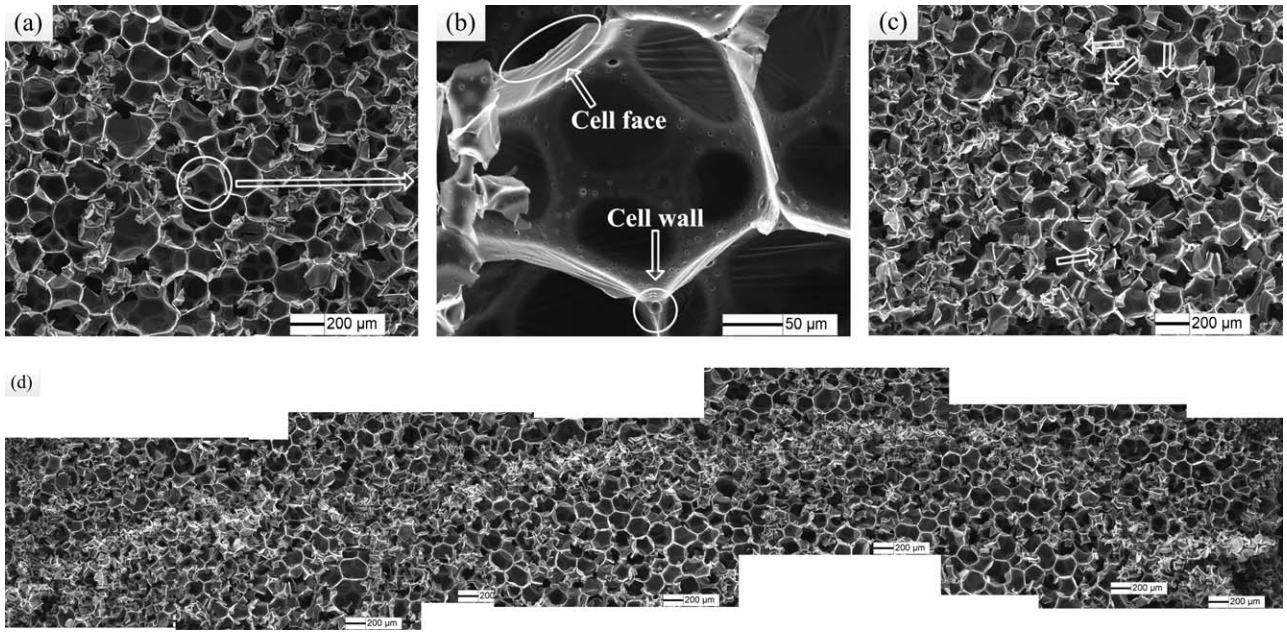

Figure 7. SEM images taken from *in situ* compression showing deformation of raw phenolic foam at different strains: (a) ~3% (× 50); (b) ~3% at high magnification (× 350), the arrow pointed to ellipse region indicates cell face and to circle region indicates cell wall; (c) ~10% (× 50), the arrows indicate the regions where cells collapse and contact; (d) ~15% (× 50).

get in touch along crack growth region. The morphology of fracture band in Figure 7(d) is evidently indicative of brittle crushing in phenolic foam which arises from the intrinsic qualities of this material, accompanied by progressive crush of cells on the boundaries. Different deformation behavior in reinforced phenolic foams is showed in Figure 8.

SEM images taken from *in situ* compression as shown in Figure 9, describe the deformation process of 0.05 wt % MWCNTs-COOH/phenolic composite foam, where big cells are ringed with some relatively small cells. Compared with phenolic foam in Figure 7, there are several distinct points in microscopic morphology of cells to be noted. When strain increases to 10%, there is no rupture taking place on the cell walls of big cells, indicating that cell walls get stronger associated with the incorporation of MWCNTs-COOH, as denoted by a, b, c in Figure 9. Furthermore, hosts of small cells, arising from good dispersion of MWCNTs-COOH in the composite foams, carry more compressive loading. This is demonstrated in Figure 9(c) where it is cells on the boundaries of the sample that bear stress and

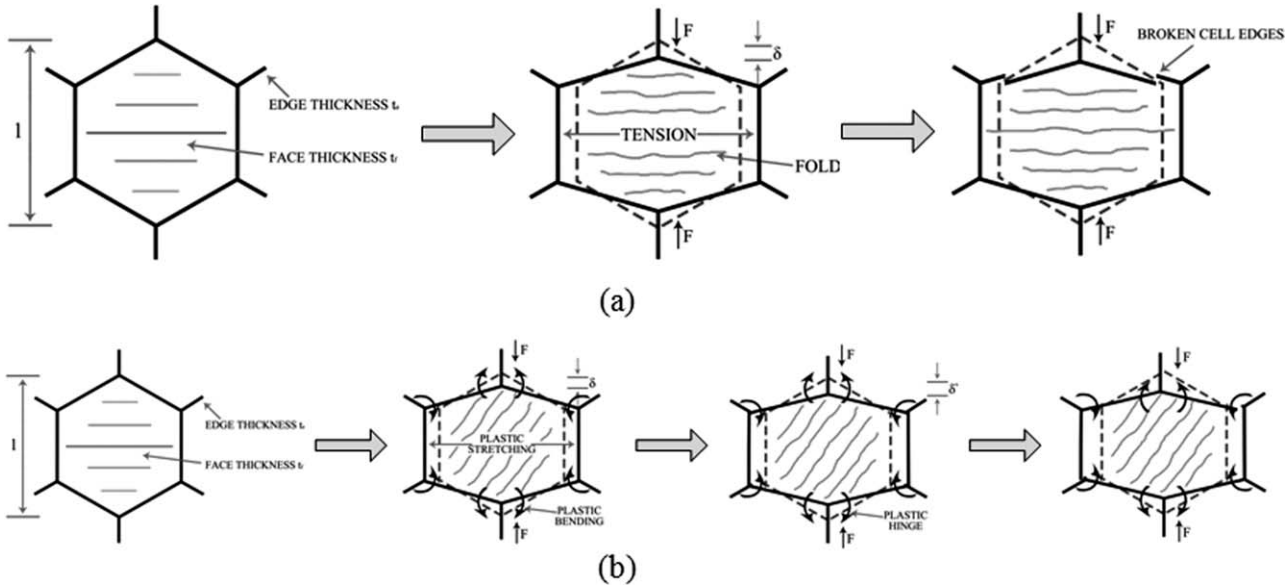

Figure 8. Illustration of different deformation behavior in reinforced phenolic foams. (a) phenolic foam. (b) MwCNTs-COOH-phenolic composite foams.

Applied Polymer SCIENCE

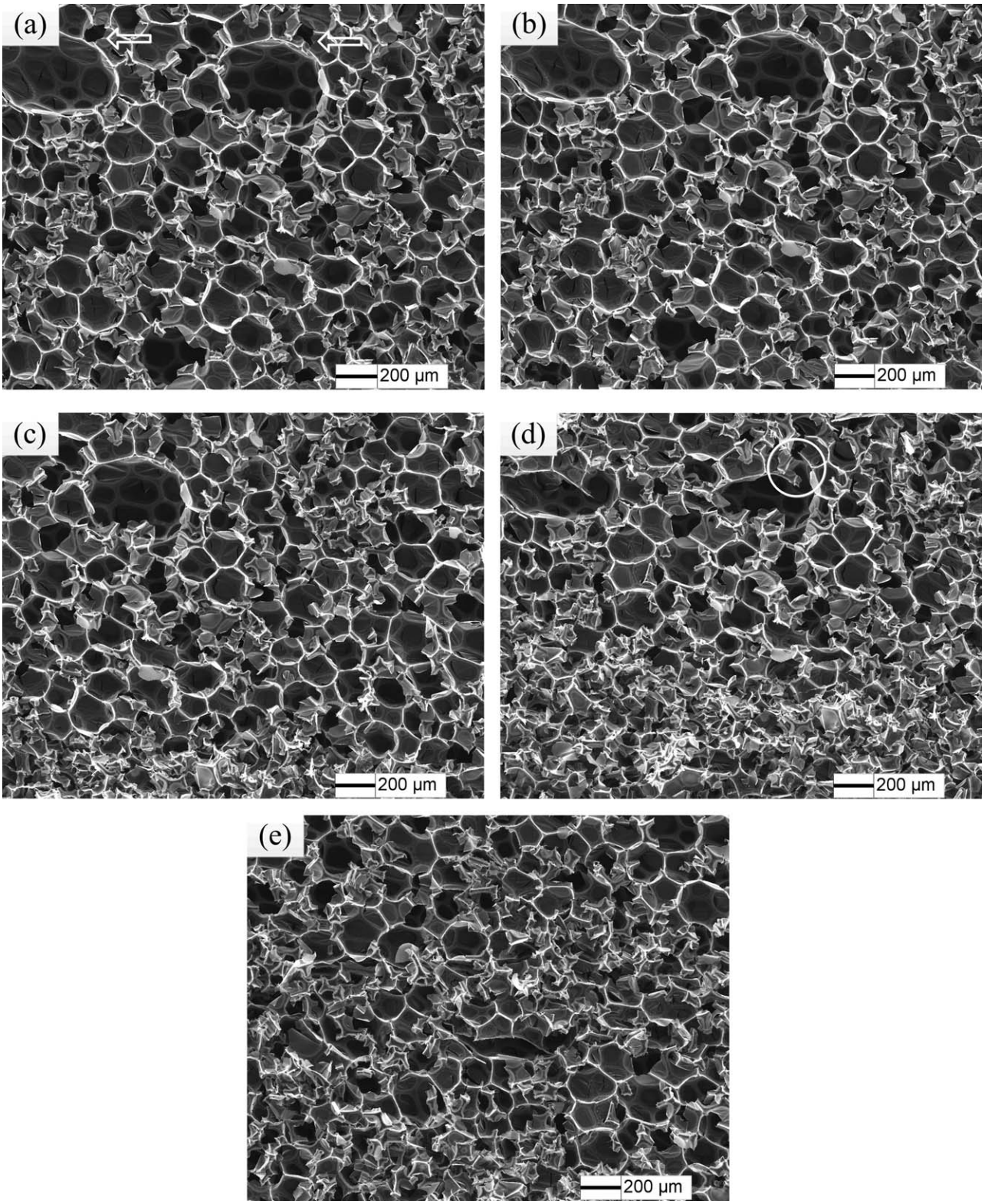

Figure 9. SEM images taken from *in situ* compression showing deformation of 0.05 wt % MWCNTs-COOH/phenolic foam at different strains under × 50: (a) ∼3%, the arrows indicate imperfections which initiate crack; (b) ∼ 6.7%; (c) ∼ 10%; (d) ∼ 13%, the circle region suggests cell-wall fracture during crushing; (e) ∼15%.

deform in a crushing pattern, whilst cells in the middle remain homogeneous. In comparison, in Figure 7(c), cell walls both on the boundaries and in the middle of the counterpart suffer from brittle rupture. In general, the composite foam still experiences progressive crushing, failing in a brittle mode, i.e., broken cell faces, as shown in Figure 9(a), induce cracks, and then

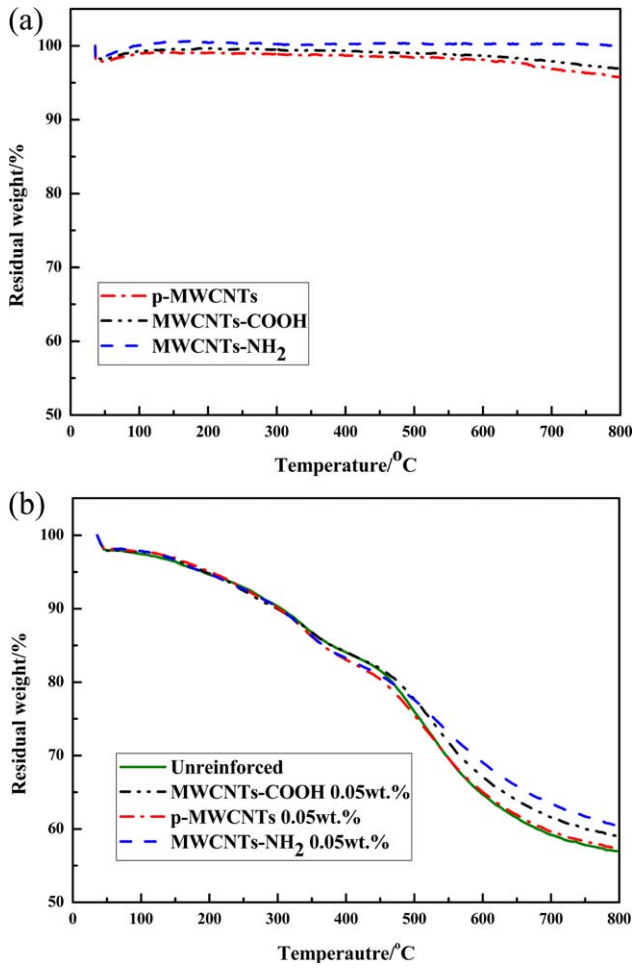

Figure 10. TGA results of (a) different kinds of MWCNTs; (b) MWCNTs/phenolic composite foams with mass fraction of 0.05 wt % and raw phenolic foam. [Color figure can be viewed in the online issue, which is available at wileyonlinelibrary.com.]

cause brittle fracture in cell walls of large cells in Figure 9(d). This phenomenon stems from the brittleness of MWCNTs/phenolic composite foam, which has a substantial solid fraction.[37] Good dispersion of MWCNTs-COOH in the composite foam reduces stress concentration as well as improves the stress transfer efficiency, thus contributes to the enhancement in the ability of deformation resistance.

Thermal Characteristics

TGA results of the unreinforced and different kinds of MWCNTs reinforced phenolic foams are presented in Figure 10 and the data concerning residual weight yield at 400, 600, and 800°C, are summarized in Table III. In Figure 10(a), it can be seen that MWCNTs-COOH has a thermal stability which is lower than that of MWCNTs-NH_2 and slightly higher than that of p-MWCNTs as a result of variations in the surface chemical state and the structure of CNTs. Meanwhile, the introduction of MWCNTs into phenolic foams increases residual weight above 500°C, especially for MWCNTs-NH_2 [Figure 10(b)]. It can be concluded that the improvement in thermal stability for MWCNTs/phenolic composite foam is determined by the thermal stability of MWCNTs.

Table III. Results from TGA Curves of MWCNTs/Phenolic Composite Foams

	Residual weight (%)		
Foam	400°C	600°C	800°C
Raw phenolic foam	84.04	64.70	56.95
0.05 wt % MWCNTs-COOH reinforced phenolic foam	84.06	67.04	58.99
0.05 wt % p-MWCNTs reinforced phenolic foam	83.01	65.01	57.34
0.05 wt % MWCNTs-NH_2 reinforced phenolic foam	83.22	69.04	60.38

MWCNTs embedded in cell walls offer stabilizing effects to restrain the thermal motion of phenolic chains, and to hinder the flux of volatile degradation products out of cell walls.[29] Consequently, the degradation rate of phenolic foam containing MWCNTs is relatively slow.

Table IV shows the flammability results for MWCNTs/phenolic foams and raw phenolic foam. All samples maintain nonignition properties and no visible smoke could be detected. Both unreinforced and reinforced foams exhibit <7% mass loss; and the loss of mass after burning decreases slightly with MWCNTs. However, there is no pronounced improvement in flame retardancy for MWCNTs/phenolic composite foam. This might be because such small amounts of MWCNTs make impossible the formation of a protective nanotube network, which could maintain structural integrity and concurrently influence heat and mass transport in phenolic solid.[29,38]

Compared to the neat phenolic foam counterpart, MWCNTs affect the properties of phenolic foam in three ways: providing remarkable stiffening and strengthening effects via cell walls/MWCNTs junctions to achieve macroscale compressive property enhancement, increasing cell density and decreasing cell size by inducing heterogeneous bubble nucleation, and offering a stabilizing effect that slows thermal degradation to slightly improve the thermal stability and fire resistance. Therefore, the proposed method using MWCNTs is an effective way for improving the mechanical and thermal properties of brittle phenolic foam.

Table IV. Flammability Properties of MWCNTs/Phenolic Composite Foams Measured Using Vertical Burning Method

Foam	Raw phenolic foam	0.05 wt % MWCNTs-COOH reinforced phenolic foam	0.05 wt % p-MWCNTs reinforced phenolic foam	0.05 wt % MWCNTs-NH_2 reinforced phenolic foam
Loss of mass/%	6.60	6.09	6.50	6.11

CONCLUSIONS

MWCNTs/phenolic composite foams with three different types of MWCNTs, including pristine, carboxyl and amino MWCNTs were successfully manufactured with the aid of ultrasonic cavitation. SEM results show that MWCNTs/phenolic composite foam is a closed-cell structure, and that cell density increases with the increase of MWCNTs content whereas cell size decreases as a result of well-dispersed MWCNTs serving as sites to accelerate heterogeneous nucleation. Moreover, the embedment of MWCNTs in cell walls significantly enhances the compressive properties of phenolic foam via reducing sensitivity to induce crack, diminishing the crack propagation rate, and delaying catastrophic collapse of cell walls. This phenomenon is verified by *in situ* quasistatic compression test inside SEM. The addition of 0.05 wt % MWCNTs-COOH increases the specific strength of foam by 31%, which is the maximum improvement using MWCNTs in this study. A marginal enhancement in thermal stability and flame-retardant property of the composite foam is observed with the incorporation of various MWCNTs, which results from high thermal stability and the stabilizing effect of MWCNTs on phenolic foam under elevated temperature.

ACKNOWLEDGMENTS

The financial support of this work by the National Natural Science Fund Program of China (Grant No. 51103003) is gratefully acknowledged.

REFERENCES

1. Papadopoulos, A. *Energ. Buildings* **2005**, *37*, 77.
2. Landrock, A. H. Handbook of Plastic Foams: Types, Properties, Manufacture, and Applications; William Andrew: New York, **1995**; Vol. *2*, p 183.
3. Auad, M. L.; Zhao, L.; Shen, H.; Nutt, S. R.; Sorathia, U. *J. Appl. Polym. Sci.* **2007**, *104*, 1399.
4. Wang, L. Y.; Gai, G. Q.; Yu, H. Y.; Liu, W. L. *Adv. Mater. Res.* **2012**, *415*, 1508.
5. Smith, S. B. Thermocell Development Ltd. U.S. Patent 4,390,641, **1983**.
6. Desai, A. Fiber Reinforced Hybrid Phenolic Foam, Ph.D. Thesis, University of Southern California, Los Angeles, **2008**.
7. McGrath, R. D.; Murphy, J. G.; Mitchell, P. R.; Koppernaes, C. C. Owens-Corning Fiberglas Technology Inc. US Patent 5,286,320, **1994**.
8. Shen, H.; Lavoie, A. J.; Nutt, S. R. *Compos. A Appl. S.* **2003**, *34*, 941.
9. Rader, S. L. Jiffy Foam, Inc. U.S. Patent 5,514,725, **1996**.
10. Kako, Y.; Kiguga, T.; Sanuki, T. Sumitomo Durez Company, Ltd. US Patent 4,131,582, **1978**.
11. Tun, H. Phenolic Foam Toughed with Glutaraldehyde. M.Sc. Thesis, Beijing University of Chemical Technology: Beijing, **2008**.
12. Heitmann, G. A.; Trosper, M. F., Jr. Johns-Manville Co. US Patent 4,169,915, **1979**.
13. Rangari, V. K.; Hassan, T. A.; Zhou, Y.; Mahfuz, H.; Jeelani, S.; Prorok, B. C. *J. Appl. Polym. Sci.* **2007**, *103*, 308.
14. Okuno, K.; Woodhams, R. *J. Cell. Plast.* **1974**, *10*, 237.
15. Shen, H.; Nutt, S. *Compos. A Appl. S.* **2003**, *34*, 899.
16. Desai, A.; Auad, M. L.; Shen, H.; Nutt, S. R. *J. Cell. Plast.* **2008**, *44*, 15.
17. Basbagill, J. P. Fiber Reinforced Phenolic Foam: Climate Effects on Mechanical Properties and Building Applications in Northern Thailand. M.Sc. Thesis, University of Southern California: Los Angeles, **2008**.
18. Esawi, A. M. K.; Farag, M. M. *Mater. Des.* **2007**, *28*, 2394.
19. Paradise, M.; Goswami, T. *Mater. Des.* **2007**, *28*, 1477.
20. Zeng, C.; Hossieny, N.; Zhang, C.; Wang, B. *Polymer* **2010**, *51*, 655.
21. Chen, L.; Ozisik, R.; Schadler, L. S. *Polymer* **2010**, *51*, 2368.
22. Chen, L.; Schadler, L. S.; Ozisik, R. *Polymer* **2011**, *52*, 2899.
23. Park, K. W.; Kim, G. H. *J. Appl. Polym. Sci.* **2009**, *112*, 1845.
24. Zhang, L.; Yilmaz, E. D.; Schjodt-Thomsen, J.; Rauhe, J. C.; Pyrz, R. *Compos. Sci. Technol.* **2011**, *71*, 877.
25. Verdejo, R.; Stämpfli, R.; Alvarez-Lainez, M.; Mourad, S.; Rodriguez-Perez, M.; Brühwiler, P.; Shaffer, M. *Compos. Sci. Technol.* **2009**, *69*, 1564.
26. Thomassin, J. M.; Pagnoulle, C.; Bednarz, L.; Huynen, I.; Jerome, R.; Detrembleur, C. *J. Mater. Chem.* **2008**, *18*, 792.
27. Yang, Y.; Gupta, M. C.; Dudley, K. L.; Lawrence, R. W. *Nano Lett.* **2005**, *5*, 2131.
28. Kashiwagi, T.; Grulke, E.; Hilding, J.; Groth, K.; Harris, R.; Butler, K.; Shields, J.; Kharchenko, S.; Douglas, *J. Polymer* **2004**, *45*, 4227.
29. Kashiwagi, T.; Du, F.; Douglas, J. F.; Winey, K. I.; Harris, R. H.; Shields, J. R. *Nat. Mater.* **2005**, *4*, 928.
30. Cipiriano, B. H.; Kashiwagi, T.; Raghavan, S. R.; Yang, Y.; Grulke, E. A.; Yamamoto, K.; Shields, J. R.; Douglas, J. F. *Polymer* **2007**, *48*, 6086.
31. Zhu, L. Prepatration and Flame Retardant Insulation Properties of Phenolic Foam Composites. M.Sc. Thesis, Beihang University: Beijing, **2011**.
32. Chen, X.; Lu, Y.; Zhang, X.; Zhao, F. *Mater. Des.* **2012**, *40*, 497.
33. Saha, M.; Kabir, M. E.; Jeelani, S. *Mater. Sci. Eng. A Struct.* **2008**, *479*, 213.
34. Wu, S. Soybean oil resin derived plastic foams and their vegetable fiber reinforced composites. Ph.D. Thesis, Sun Yat-Sen University: Guangzhou, **2008**.
35. Zhang, B. S.; Lv, X. F.; Zhang, Z. X.; Liu, Y.; Kim, J. K.; Xin, Z. X. *Mater. Des.* **2010**, *31*, 3106.
36. Gibson, L. J.; Ashby, M. F. Cellular Solids: Structure and Properties; Cambridge University Press: Cambridge, **1999**.
37. Yeh, M. K.; Tai, N. H.; Liu, J. H. *Carbon* **2006**, *44*, 1.
38. Moniruzzaman, M.; Winey, K. I. *Macromolecules* **2006**, *39*, 5194.